



RESEARCH ARTICLE

PLASMA PROCESSES
AND POLYMERS

Insight into peculiar adhesion of cells to plasma-chemically prepared multifunctional “amino-glue” surfaces

Martina Buchtelová¹ | Lucie Blahová¹ | David Nečas¹ | Petra Křížková² |
Jana Bartošíková² | Jiřina Medalová² | Zdeňka Kolská³ | Dirk Hegemann⁴  |
Lenka Zajíčková^{1,5} 

¹Plasma Technologies for Materials, Central European Institute of Technology – CEITEC, Brno University of Technology, Brno, Czech Republic

²Department of Experimental Biology, Faculty of Science, Masaryk University, Brno, Czech Republic

³Faculty of Science, J.E. Purkyně University, Ústí nad Labem, Czech Republic

⁴Empa, Swiss Federal Laboratories for Materials Science and Technology, Advanced Fibers, St. Gallen, Switzerland

⁵Department of Condensed Matter Physics, Faculty of Science, Masaryk University, Brno, Czech Republic

Correspondence

Lenka Zajíčková, Plasma Technologies for Materials, Central European Institute of Technology – CEITEC, Brno University of Technology, Purkyňova 123, Brno 612 00, Czech Republic.

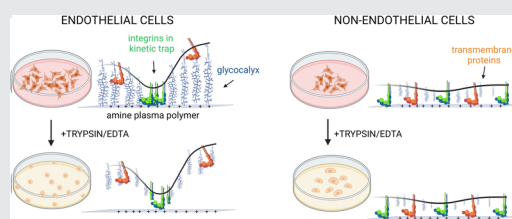
Email: lenkaz@physics.muni.cz

Funding information

Ministerstvo Školství, Mládeže a Telovýchovy, Grant/Award Numbers: CZ.02.2.69/0.0/0.0/19_073/0016948, LM2018110, LM2018127; Grantová Agentura České Republiky, Grant/Award Number: 21-12132J

Abstract

Plasma polymers (PPs) can easily modify material surfaces to improve their bio-applicability due to match-made surface-free energy and functionality. However, cell adhesion to PPs typically composed of various functional groups has not yet been fully understood. We explain the origin of strong resistance to trypsin treatment previously noted for nonendothelial cells on amine PPs. It is caused mainly by nonspecific adhesion of negatively charged parts of transmembrane proteins to the positively charged amine PP surface, enabled by thin glycocalyx. However, endothelial cells are bound primarily by their thick, negatively charged glycocalyx and sporadically by integrins in kinetic traps, both cleaved by trypsin. Cell scratching by atomic force microscopy tip confirmed the correlation of trypsin resistance to the strength of cell adhesion.



KEYWORDS

amine plasma polymer, carboxyl plasma polymer, cell adhesion, glycocalyx, nonspecific adhesion

This is an open access article under the terms of the Creative Commons Attribution-NonCommercial-NoDerivs License, which permits use and distribution in any medium, provided the original work is properly cited, the use is non-commercial and no modifications or adaptations are made.

© 2023 The Authors. *Plasma Processes and Polymers* published by Wiley-VCH GmbH.

1 | INTRODUCTION

Diseases, injuries, and birth defects are, and always have been, a part of human existence. At first, people tried to cure or replace incurable defects with natural materials.^[1] Later on, they came up with the idea of the transplantation of tissues and organs. However, the lack of good immunosuppression and the inability to monitor and control rejection, as well as a severe shortage of organ donors, limited their efforts. But simultaneously, it motivated the development of other alternatives, that is, tissue engineering.^[2,3] One of the main efforts in tissue engineering is to find a suitable material to create a scaffold for cell growth. High biocompatibility, appropriate biodegradation, and low immunogenicity are required for scaffolds. The ideal biomaterial further promotes cell–cell interaction and development and exhibits appropriate mechanical and physical properties. Recent findings indicate that another important requirement is the proper extracellular matrix (ECM) environment, which contains proteins, cytokines, and other substances that regulate cellular functions such as migration, proliferation, and differentiation. Biomaterials should appropriately simulate the ECM.^[4]

Initial interactions of cells with biomaterials are influenced by chemical composition, surface energy, pore presence and size, roughness, and geometry of top surface layers, which are in direct contact with body fluid and cells. This interaction starts with the wetting of the surface by water, the adsorption of proteins from the blood or sera, and only then it is possible to attach the cells.^[5] Synthetic biodegradable polymers, such as polycaprolactone (PCL), poly(L-lactic acid), poly(glycolic acid), poly(lactic-co-glycolic acid), are promising candidates for biomaterial development because they can be easily electrospun in the form of nanofibers resembling the structure of ECM offering more controllable nanofibrous morphology than natural polymers.^[6] However, it is necessary to overcome the hydrophobicity of synthetic polymers, which is further increased by a topological effect of nanofibrous architecture.^[7] The introduction of surface groups such as amino groups, carboxyls, hydroxyls, or anhydrides increases the surface-free energy making the electrospun mat hydrophilic, which in turn improves cell adhesion. Furthermore, the functional groups can mediate the immobilization of proteins, enzymes, growth factors, or drugs.^[6] At the same time, long-term stability of surface functionalization can be attained by depositing a plasma polymer (PP) thin film, while the bulk properties of the material remain intact.^[8] PPs containing carboxyl (–COOH) or primary amino (–NH₂) groups are often proposed for bioapplications.^[7,9,10]

The nature of cell adhesion to the substrate surface has a major impact on cell function and tissue development, as signaling cascades triggered by cell adhesion can regulate several events such as embryogenesis, tissue differentiation, and cell migration.^[11] Adherence of cells to ECM is mainly provided by focal adhesion, the subcellular complex that mediates the connection of cytoskeleton and surface receptors on the cell membrane, called integrins, which selectively bind to adhesion proteins such as laminin, fibronectin, and vitronectin occurring in ECM, and maintain a vital connection with intracellular skeleton and thus affect cytokinetic processes.^[12] In our previous study,^[13] we observed a unique phenomenon related to cell adhesion—myoblasts (C2C12), fibroblasts (LF), keratinocytes (HaCaT), smooth muscle cells (VSMC), which we collectively called nonendothelial cells, resisted trypsin/EDTA treatment (used routinely for cell detachment during passaging) when cultivated on amine PPs, whereas endothelial cells (HSVEC, HUVEC, and CPAE) were detached. Thus, for nonendothelial cells, the plasma-chemically prepared amine surfaces function as “amino-glue.” Importantly, compared to the chemical preparation of “amino-glue,” for example, the preparation of polydopamine-based coating,^[14] plasma-chemical preparation is much less time-consuming.

EDTA treatment chelates ions that are necessary for the integrins' proper function, and trypsin cleaves cell adhesion mediating proteins, mainly extracellular parts of integrin (cleaves C-terminal to arginine and lysine residues).^[15,16] Besides the standard integrin-based mechanism, a significant contribution of nonspecific adhesion through electrostatic interactions is applied on “amino-glue” surfaces. As proposed,^[13] the nonspecific interactions between the material surface and cells could be mediated by many factors, for example, the negatively charged glycocalyx, which is a complex of proteoglycans, glycoproteins, and glycosaminoglycans surrounding the cell membrane.^[17,18] Another factor in nonspecific adhesion may be tissue transglutaminase (TG) activity. TGs are a family of Ca²⁺-dependent enzymes that covalently crosslink proteins by forming amide bonds between glutamines and ϵ -amino groups of lysine. TGs can crosslink nearly all ECM proteins by post-translational modification through transamidation or deamidation and were reported to have also cell adhesion activity.^[19,20] Nonspecific cell adhesion can also be affected by the composition of the cell culture media.^[21]

This study addressed two main questions: which of the above-mentioned mechanisms causes nonspecific binding to amine PPs and trypsin resistance of nonendothelial cells and whether the increased trypsin resistance is directly correlated to increased cell

adhesion. The strength of adhesion was assessed by cell scratching by atomic force microscopy (AFM), which measures the total strength of both integrin-mediated and nonspecific cell adhesion. The type of nonspecific interaction that causes cell resistance to trypsin/EDTA was elucidated by analyzing the activity of TGs and the role of the glycocalyx. The work aims to explain the nature of cell-type specific adhesion to the “amino-glue” surfaces.

2 | MATERIALS AND METHODS

2.1 | Preparation and characterization of PPs

PPs with different content of nitrogen and oxygen were prepared by the plasma-enhanced chemical vapor deposition (PECVD) in radio frequency (13.56 MHz) discharge with a capacitive coupling on standard polystyrene culture dishes (TPP, Switzerland). The PP type selection was based on previous detailed studies of PECVD from cyclopropylamine (CPA) vapors mixed with Ar (for amine PPs),^[13,22,23] and PECVD from the mixture of ethylene (C_2H_4) and carbon dioxide (CO_2) for carboxyl PPs.^[24–26]

Three types of amine PPs were deposited at a pressure of 50 Pa and an Ar flow rate of 28 sccm; the flow rate of CPA was held at 2 sccm. In two cases, the radio frequency (RF) discharge was operated in the pulsed mode using the duty cycle (DC) of 33% and the repetition frequency of 500 Hz. The on-time RF power was 30 or 100 W. The third sample was prepared in continuous wave discharge (DC 100%) at the RF power of 150 W. The governing parameter related to the film properties was the average RF power, P_{av} , calculated as the on-time power multiplied by the DC. The average powers (P_{av}) corresponding to the three used deposition conditions are 10, 33, and 150 W.

The carboxyl PPs were deposited according to the procedure previously optimized on Si substrates for improved stability and surface functionality.^[24,25] The C_2H_4 gas flow rate was held constant at 4 sccm. First, a highly crosslinked base layer was prepared at the RF power and the CO_2/C_2H_4 flow rate ratio of 70 W and 2:1, respectively. Then a less crosslinked layer with more functional groups was deposited on the top at 30 W and the CO_2/C_2H_4 ratio of 6:1 by enhancing the plasma oxidation process. On the Si substrate, the PP coating had a gradient structure, a 19 nm well-crosslinked base layer, and a 1 nm oxygen-rich top layer, maintaining high hydrophilicity.^[24]

PPs were characterized for their chemical composition and chemical bonds by X-ray photoelectron spectroscopy (XPS). The surface analysis was carried out using an Axis Supra (Kratos Analytical) spectrometer. The elemental composition was quantified from the high-resolution spectra of each element, and high-resolution C1s spectra were fitted to obtain individual components using CasaXPS software (version 2.3.24) after subtracting the Shirley-type background, employing Gaussian–Lorentzian (G–L) peaks with a fixed G–L percentage of 30%. The values of the binding energies of the C environment were taken from the literature. In the case of amine PPs, the C1s peak was fitted with a sum of five components: aliphatic hydrocarbon groups (CH_x , C–C) at 285.0 eV, amino groups bonded to carbon (C– NH_x) at 285.9 eV, imine or nitrile groups (C=N/C \equiv N) at 286.7 eV, aldehydes/ketones or amide groups (C=O/N–C=O/N–C–O) at 287.9 eV, and carboxyl/ester groups (C(O)OR) at 288.9 eV.^[27] The quantification of primary amino groups was performed by 4-trifluoromethyl benzaldehyde (TFBA, purity 98%, Sigma Aldrich) derivatization.^[28,29] Due to the high sensitivity of TFBA to moisture and oxygen, the reaction was carried out in an Ar atmosphere. The amine PP layers were placed in the glovebox immediately after the preparation. The glovebox chamber was pumped down with a membrane pump and filled with Ar. The procedure was repeated three times to avoid the residue of oxygen and moisture. Each sample was placed on the top of the glass beads inside the 100 mL flask and 0.1 mL of TFBA was dropped in such a way as to avoid the contact of liquid with the sample surface. Then the flask was closed and the reaction proceeded for 90 min. The density of primary amino groups (NH_2) expressed in at.% was calculated from the fluorine and carbon atomic concentrations measured by XPS similarly as reported in the literature.^[30,31] For the identification of functional groups in carboxyl PPs, a model composed of four components was used: aliphatic hydrocarbon (CH_x , C–C) at 285.0 eV, hydroxyl/ether (C–O) at 286.4 eV, aldehyde/ketone (C=O) at 287.8 eV, and carboxyl/ester (C(O)OR) at 289.0 eV.^[24]

The water contact angle (WCA) was measured by the sessile drop technique^[27] with the See System (Advex Instruments), enabling the observation of a solid–liquid meniscus using a CCD camera. The contact angles were determined from the CCD snapshots.

In this work, we added two other important physico–chemical characteristics of the films that can impact the cell-surface interactions, surface charge (ζ -potential), and surface stiffness. Electrokinetic analysis (ζ -potential measurement) was performed on the device SurPASS using the adjustable gap cell recommended for the determination of the ζ -potential of planar samples (Anton Paar, Austria). Due to the requirements of

ζ -potential measurement, amine, and carboxyl PPs were deposited on PET foil (product No. ES301230, thickness 0.023 mm, Goodfellow Ltd). Two samples of the same surface were fixed on two holders; the size of the samples was $2 \times 1 \text{ cm}^2$. Measurements were carried out in a cell with an adjustable gap of about $100 \mu\text{m}$, at room temperature, atmospheric pressure, and constant pH 6.4 with an experimental error of 5%. For the determination of ζ -potential, the streaming current method and the Helmholtz-Smoluchowski equation were used.^[32,33]

PP stiffness was measured using a Dimension Icon AFM microscope (Bruker Nano GmbH). Force–distance curves were acquired using a TESPA-V2 probe (Bruker Nano GmbH) in at least 18 locations at each sample, three curves $5 \mu\text{m}$ apart per location. They were converted to force separation and fitted in the Nanoscope Analysis software using a standard polystyrene sample for modulus calibration.

2.2 | Cell cultivation

Cultivation of human skin fibroblasts (LF), human keratinocytes (HaCaT), vascular smooth muscle cells (VSMC), human endothelial cells (HSVEC), and bovine endothelial cells (CPAE) took place in constant incubator conditions (37°C , air atmosphere with 5% CO_2 , and 95% humidity). All of them, except HSVEC, were cultivated in DMEM (Dulbecco's modified Eagle's medium, high glucose, Gibco, Thermo Fisher Scientific) with the addition of 10% fetal bovine serum (FBS, Gibco, Thermo Fisher Scientific), 1.2 mM L-glutamine (Gibco, Thermo Fisher Scientific) and 100 U/ml Penicillin/Streptomycin (HyClone, Thermo Fisher Scientific). The HSVEC cells were cultivated in special media for endothelial cells Endothelial Cell Growth Medium 2 with the following supplements: 5% FCS, Human Epidermal Growth Factor, Vascular Endothelial Growth Factor, basic Fibroblast Growth Factor, R3 Insulin-like Growth Factor-1, Ascorbic acid, Hydrocortisone, Heparin (PromoCell), and 100 U/ml Penicillin/Streptomycin (HyClone, Thermo Fisher Scientific). The cell cultures in all the experiments were used in the range of 10 passages. VSMC cells are originally primary culture but with extended cultivation till the 25th passage, and we used cell passages 15–25. For endothelial HSVEC cells, only the first six passages were used for experiments as they are primary cultures.

Cells in the stock passage and control dishes were cultured in standard laboratory tissue culture dishes ($40 \times 10 \text{ mm}$, volume 2 mL, TPP, Merck, Kenilworth). The same culture dishes coated with amine and carboxyl PPs were used for the experiments. The properties of PPs prepared in culture dishes are the same as for planar

substrates, as demonstrated by Michlíček et al.^[34] The cells were seeded on all the tested types of dishes in the concentration of $0.5\text{--}1 \times 10^5$ cells per dish. During passaging, phosphate-buffered saline (PBS; pH 7.4) was used to rinse all types of cells. Then, they were enzymatically released from the surface by trypsin/EDTA (ethylene-diamine tetraacetic acid, Biosera, Onsala, Sweden, product No. LM-T1706/100). HaCaT cells were pretreated for 10 min with 0.05% EDTA before exposure to trypsin (trypsinization) because of their strong adhesion to culture dishes. Inversion microscope CKX 41 (Olympus) served for visual inspection of cells during passage and experiments.

2.3 | Trypsinization

Before trypsinization, approximately 1×10^5 cells were seeded on polystyrene culture dishes and cultivated at the standard conditions as described in Section 2.2. for 24 h. After washing them with PBS, 0.5 mL of trypsin/EDTA was added, and the cells were photographed at times of 0, 10, 20, and 30 min by using the IX51 microscope equipped with the digital camera CAMEDIA (both Olympus). To take pictures of attached cells only, the trypsin/EDTA containing detached cells was replaced with the fresh trypsin/EDTA. Cell resistance to the enzymatic activity of trypsin was evaluated as the detachment of cells from the PP coated versus control culture dishes.

To evaluate the effect of glycocalyx on cell adhesion, endothelial cells CPAE and HSVEC were incubated in three differently modified culture media that should degrade their glycocalyx. First, cells were starved by cultivation in the serum-free medium DMEM:F12 with the addition of ITS supplement^[35,36] (containing only insulin, transferrin, and selenium, all from Gibco BRL, Chemos CZ, Prague, Czech Republic). Second, the effect of the starvation was enhanced by the inhibitor of the glycosylation 100 ng/mL tunicamycin,^[37] and third, we increased the glycemia of DMEM media from 25 mM to 50 mM^[38] by the addition of glucose (Merck). After 5 h of incubation, the cells were trypsinized as described above.

The results were evaluated using the 1.51w Fiji SW/program (Wayne Rasband, NIH). At each condition, four field shots focused on the surface automatically adjusted for intensity, saturation, and color clarity were taken. Subsequently, the binarization of the acquired mask and its optimization were performed using image analysis tools. The results were obtained by automatic counting of particles larger than 600 pixels and in graphs given as the average number of sessile cells per field of view. For each sample, four independent measurements were done. Each time the dependence was normalized independently by dividing by the value for time $t = 0 \text{ min}$ when

trypsin was added. The variance of this value was taken into account in the variances of plotted values at other times using the standard error propagation rule.

2.4 | Assessment of TG activity by dansyl cadaverine incorporation

The activity of TGs in studied cells was assessed by fluorimetric evaluation of incorporated amine donor dansyl cadaverine (Merck).^[39,40] All cells were seeded into a 96-well plate in quadruplicates in the concentration of 1×10^4 cells per well. In 12 h, the 25 μ M dansyl cadaverine was added. The fluorescence of the dansyl group incorporated by TGs was measured in cells washed by PBS in 5 h of incubation (Hidex Sense microplate reader, Hidex, Turku, Finland; ex. 330/80 nm, em. 535/20 nm).

Fluorescence of dansyl groups, spontaneously, adhered to the well surface (wells with dansyl cadaverine without cells) was subtracted from the results and they were normalized by dividing results by value of cells autofluorescence (wells with cells without dansyl cadaverine). The variance of this value was taken into account in the variances of plotted values of other cell lines using the standard error propagation rule.

2.5 | Western blot analysis

Western blot analysis was performed to identify protein expression of proteins involved in adhesion and connection with surface, especially integrins, and cadherins. Briefly, cells were washed twice with PBS (pH 7.4), lysed in lysis buffer containing 1% SDS, 5% β -mercaptoethanol, 0.002% bromophenol blue, and 0.06 M TRIS HCl (pH 6.8). The equal amounts of proteins measured by the DC Protein Assay (5000111, Bio-Rad) were denatured by boiling and sonification, and a protease inhibitor cocktail (11836145001, Roche) was added. Electrophoresis in 8% SDS-polyacrylamide gel followed. The proteins were transferred to nitrocellulose Immobilon-P PVDF Membrane (IPVH00010, Millipore) and immunoblotted using monoclonal antibodies: CD 29—integrin β 1 (712591), CD 49b—integrin α 2 (7125511), CD 49e—integrin α 5 (7125995), CD 51—integrin α V (7125983), CD 61—integrin β 3 (7125997), CD 11a—integrin α L (7125502), fibronectin (7125988) all of them from BD Biosciences (Becton, Dickinson, and Company), N cadherin (59987), VE cadherin (9989), M cadherin (398107), integrin α 7 (515716), all of them from Santa Cruz Biotechnology, Inc., tubulin α (5335), β -catenin (2009), both from Cell Signaling Technology, active β -catenin (5665) from

Merck Millipore and E cadherin (1336510) from SONY Biotechnology at dilutions of 1:1000. Then, corresponding HRP-conjugated secondary antibodies at dilutions of 1:5000 were used and detected on Fusion SL imaging system (Vibler) using Immobilon Western Chemiluminescent HRP Substrate (Merck, WBKLS0500).

2.6 | Cell stiffness and scratching

Cell stiffness was measured using AFM microscope NanoWizard 3 (Bruker Nano GmbH) in Force Mapping mode.^[41] The measurement of cell stiffness was performed by nanomechanical mapping, which resulted in a force map of 16×16 points. The force curves were evaluated in the AtomicJ,^[42] which offers the possibility to specify selected parameters of the tip with which the measurement took place. A truncated pyramid-shaped silicon tip with a radius of 5 μ m, height of 10–15 μ m, and angle-to-edge of 18° (Figure 1a) was used for the measurement. When evaluating the force map of the cell, only the force curves from the center of the cell were considered, thus eliminating the influence of the base material. The region of interest (ROI) function of AtomicJ was used to select a suitable cell area.

The cell adhesion to the surfaces was also studied using the AFM microscope NanoWizard 3 (Bruker Nano GmbH) but in the Imaging mode.^[41] The strength of adhesion was determined as the force required to scratch the cell from the surface of the culture dish. Using a truncated pyramid-shaped tip (Figure 1a), the tip moved across the cell until it was scratched off the surface. At first, the adhesion complexes at the edge of the cell were disrupted (Figure 2b); with increasing force, the disruption increased (Figure 2c) and then the cell was completely torn off the surface (Figure 2d). This force value was recorded as the force required to completely scratch the cell from the surface.

After measuring cell stiffness and cell scratching, SEM micrographs were taken by using SEM/FIB microscope FEI Versa3D to inspect the tip. The tip remained unchanged after the measurement; only the remains of cells are visible (Figure 1b).

3 | RESULTS

3.1 | Surface properties influencing the cell-surface interaction

The chemical structure of the amine films (measured by XPS) was thoroughly described in previous

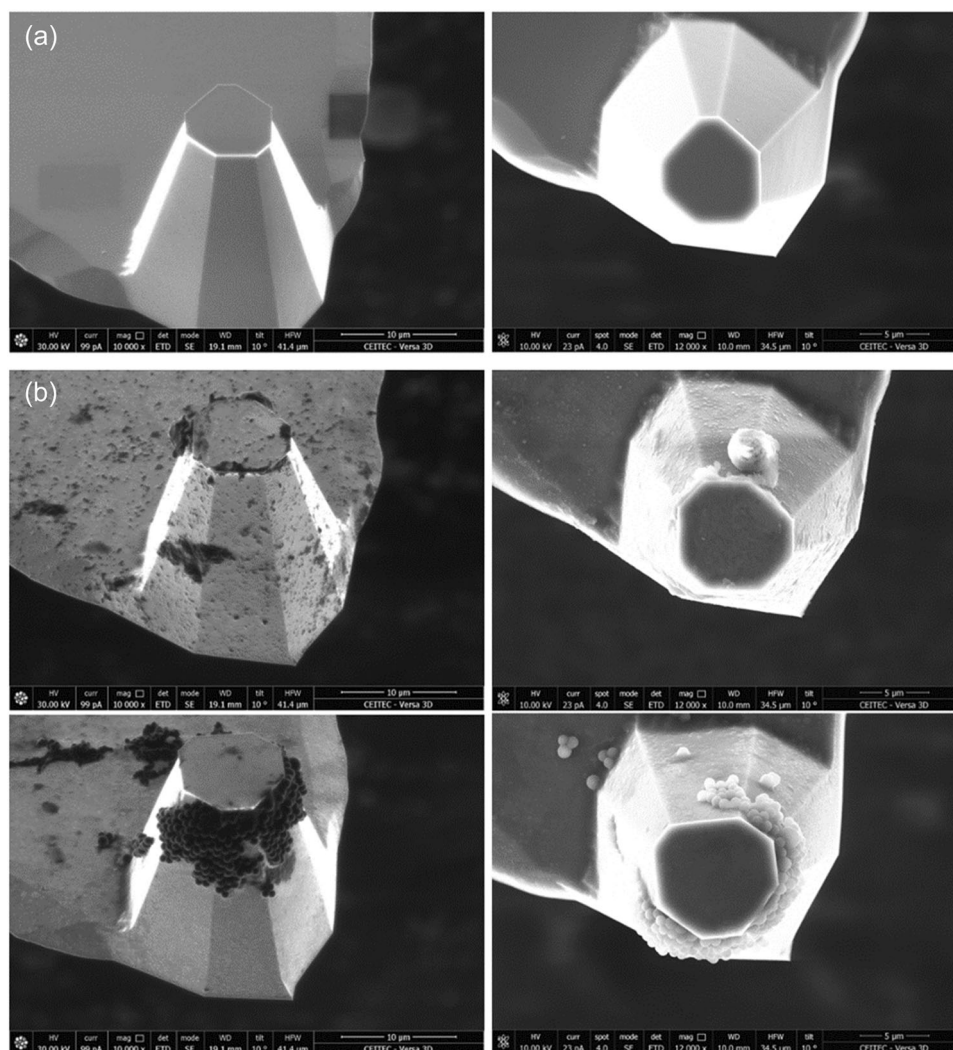


FIGURE 1 Scanning electron microscope (SEM) micrographs of truncated pyramid-shaped tip used to measure cell stiffness and scratching. (a). Tip before measurement. (b) Tip after measurement with the remains of cells.

publications.^[13,22] Regardless of the deposition conditions, the nitrogen content was higher than 10 at.% in all amine PPs (Figure 3b). A lower power invested into the plasma polymerization process led to higher retention of the functional group present in the precursor, which was confirmed by chemical derivatization. The PP film deposited at the lowest $P_{av} = 10$ W (30 W, 33%) possessed the highest number of primary amino groups (3 at.%) and also nitrogen functionalities in total (19 at.%). The nitrogen content decreased with increased P_{av} in favor of carbon (Figure 3a, atomic fraction of C). The same trend was followed by imine and nitrile groups ($C=N/C\equiv N$) but, surprisingly, not by amino groups ($C-NH_x$). The content of all amino groups was similar for all the deposition conditions—around 12 at.%. The XPS analyses of the amine PPs were intentionally performed after 14 days of air exposure, that is, at the same aging time as the cell experiments. Oxygen content

originating from the oxidation of amine PPs was 5 at.% for the PP prepared at the maximum $P_{av} = 150$ W (150 W, cont.) and lower for the rest.

The carboxyl PP had smaller carbon content compared to amine PPs (Figure 3a) due to a higher oxygen content of around 20 at.%. Although the polymers contained a large amount of oxygen functional groups and are called “carboxyl,” the amount of carboxyl functional groups was just slightly above 4 at.%. More represented functional groups were hydroxyls/ethers ($C-O$; 12.4 at.%) and aldehydes/ketones ($C=O$; 7.4 at.%) (Figure 3b). The carboxyl PPs also contained a small amount of nitrogen, which is probably related to air leakage. In the reactor where the carboxyl PPs were prepared the air leakage is typically 0.1 sccm or less, depending on how precisely the top electrode is placed.

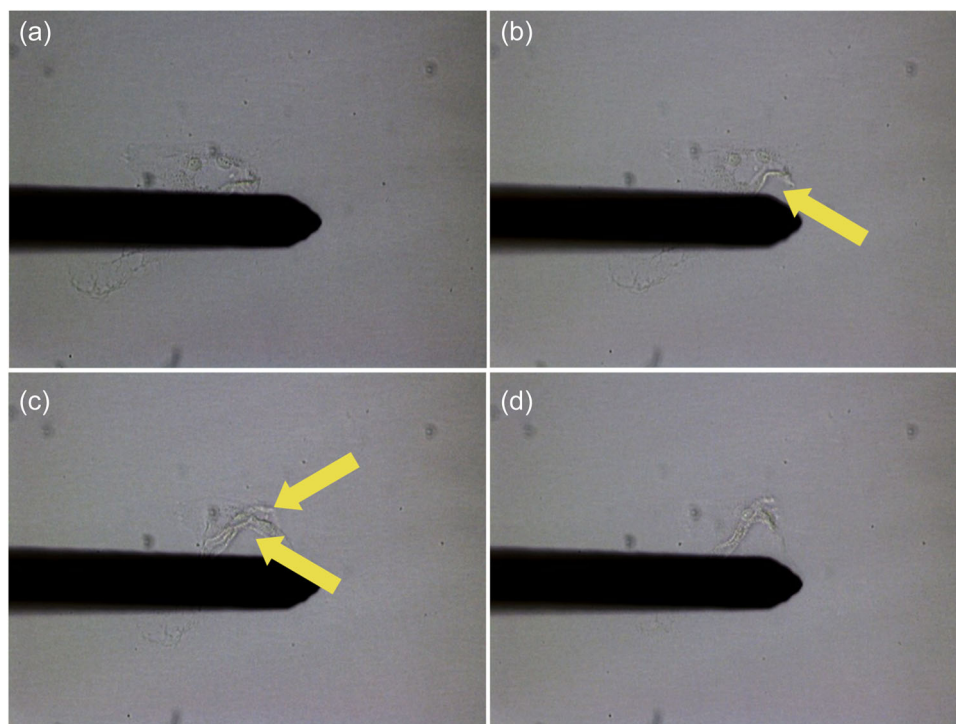


FIGURE 2 Scheme of cell scratching. (a) Cell before scratching. (b) Cell started to detach from the surface at the edges. (c) Cell almost detached from the surface. (d) Cell after scratching.

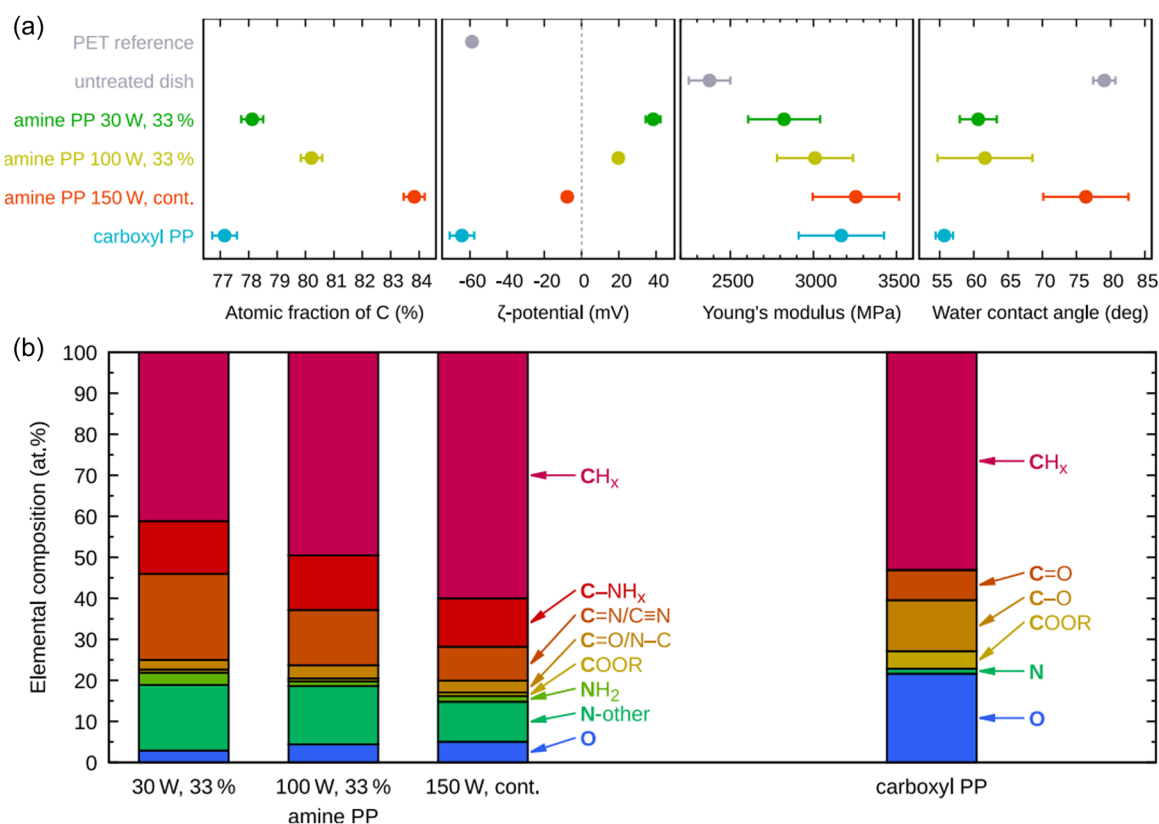


FIGURE 3 (a) Analyses of surface properties—atomic fraction of carbon content, ζ -potential (at pH 6.4), Young's modulus, and water contact angle. (b) Detailed analyses of chemical composition by X-ray photoelectron spectroscopy (XPS), bold font denotes the corresponding element and its high-resolution spectrum fitting (red—carbon; green—nitrogen; blue—oxygen).

The chemical composition of the films was well reflected by electrokinetic analyses determining the surface charges (ζ -potential) of studied surfaces. As demonstrated in Figure 3a (2nd graph), the ζ -potential was the highest for the layer prepared at 30 W, 33%, which had the highest nitrogen content and positively charged amino and other nitrogen-containing groups. For the layer at 150 W, cont., which had the lowest nitrogen content and the highest content of negatively charged oxygen-containing groups (Figure 3b), the ζ -potential was the lowest among the amine PPs. However, this PP still contained a significant amount of nitrogen and amino functional groups compared to the PET reference. Therefore, the ζ -potential was less negative than the PET reference.

In contrast, carboxyl PP, which contains predominantly oxygen and negatively charged oxygen functional groups, has the ζ -potential value even lower than for the PET reference. It corresponds well with XPS results, the higher amount of nitrogen groups, and the much positive ζ -potential. These changes could have been accompanied by changes in surface stiffness. As shown in Figure 3a (3rd graph), the stiffness of amine PPs deposited into polystyrene culture dish is constantly increasing with increasing P_{av} . The stiffness of carboxyl PPs is, within the measurement errors, comparable to the stiffness of 150 W, cont. amine PP.

3.2 | Trypsinization

In the previous publication,^[13] we described the differences in trypsin resistance for several cell types on dishes coated with amine PPs. Here, we expanded the study with dishes coated with carboxyl PPs (Figure 4). For comparison, the previously published results of trypsinization on amine PPs are also shown in Figure 4. As demonstrated in Figure 4, nonendothelial cells (HaCaT, VSMC) show strong resistance to trypsin on amine PPs, as the trypsinization of exposed cleavage sites only makes the cell roundish, not detached (Supporting Information: Figure S1). Interestingly, their resistance is only weak when growing on carboxyl PPs. This difference is the most pronounced for VSMC that remained on amine PPs even after 30 min of trypsin treatment. They were alive although a bit roundish. On carboxyl PP, their resistance was similar to the control dish, where almost all cells were detached from the surface after 10 min of trypsin treatment (Figure 4). HaCaT cells on carboxyl PPs behaved similarly, just a bit delayed—there were no cells attached after 20 min of trypsin treatment. Thus, nonendothelial cells were attached strongly to amine PPs but adhered weakly to carboxyl PPs (Figure 4). Since this phenomenon has not been shown on carboxyl surfaces, we can indeed call it the “amino-glue” effect, and further experiments were carried out only with amine PPs.

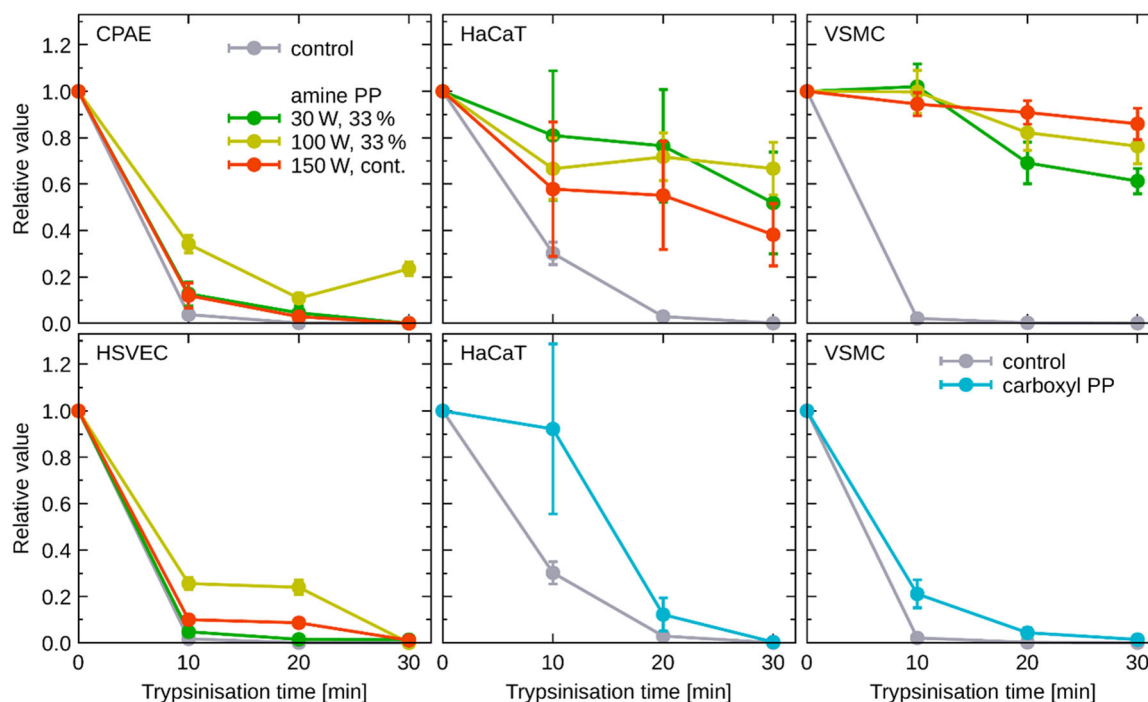


FIGURE 4 Differences between trypsinization of endothelial cells (CPAE, HSVEC) and nonendothelial cells (HaCaT, VSMC) on “amino-glue” surfaces^[13] and surfaces with carboxyl groups.

3.3 | Cell stiffness and adhesion on amine PPs

It is believed that focal adhesion plays an important role in the mechanosensing of cells upon contact with the substrate. It is recognized as the major intermedia architecture connecting the ECM and F-actin.^[43] Thus, different surface stiffness of amine PPs could be manifested in different cell stiffness. We chose HSVEC and VSMC as endothelial and nonendothelial cell representatives, respectively (Figure 4). The stiffness of the amine PPs varied slightly and was the lowest for layer

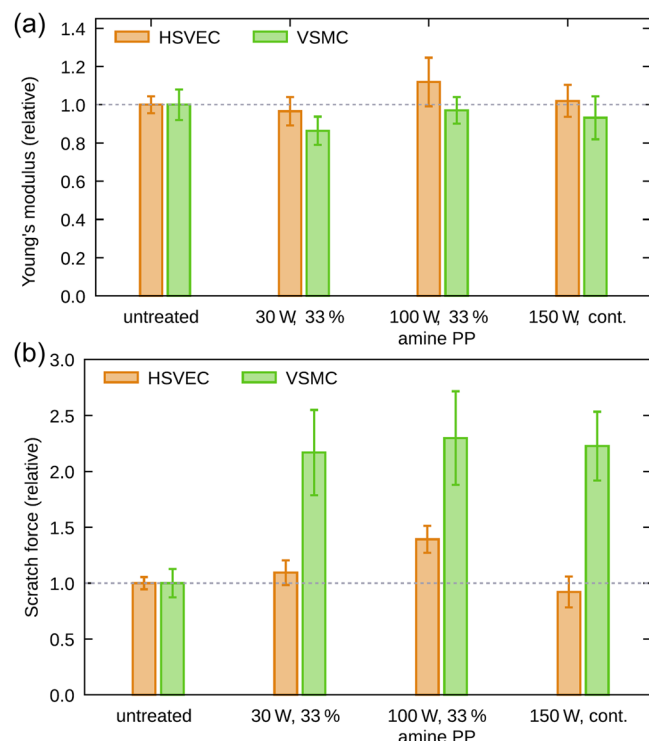


FIGURE 5 (a) Cell stiffness expressed as Young's modulus. (b) Adhesion of cells to the surface, expressed as the force necessary to detach cells from the surface by scratching.

30 W, 33%. However, the stiffness of the cells (both HSVEC and VSMC) did not change (Figure 5a).

To answer whether increased trypsin resistance of nonendothelial cells is directly related to their higher adhesion to the PP surface, cell scratch tests were performed with the two selected cell types. The relative value of the force required to scratch the cell off the surface was compared (Figure 5b). Interestingly, HSVEC showed a similar degree of adhesion to amine PPs as to the untreated control dish, except for the layer deposited at 100 W, 33%, where the adhesion was about 40% higher than on the control dish. On this surface, we also observed a slightly increased resistance of HSVEC cells to trypsin (Figure 4). In contrast, VSMCs adhered very strongly to all the amine PPs compared to the untreated control dish. The relative values are twice as high. This result confirms the assumption that the mechanism of adhesion of endothelial (HSVEC) and nonendothelial cells (VSMC) to amine PPs is different^[13] and that trypsin resistance is accompanied by higher cell adhesion.

The glycocalyx, whose morphology, thickness, and composition can differ for different cell types, may play a role in a different mechanism of cell adhesion. To verify the hypothesis about the role of different compositions and the thickness of glycocalyx in cell adhesion, three different methods inducing the glycocalyx degradation were used: hyperglycemia,^[38] starvation,^[37] and glycosylation inhibition.^[35,36] After degrading the thick and negatively charged glycocalyx of endothelial cells, they were expected to behave similarly to nonendothelial cells, that is, adhere more strongly to amine PPs. As shown in Figure 6, endothelial cells (CPAE and HSVEC) before glycocalyx degradation adhered weakly to both the control untreated surface and the amine PP deposited at 100 W, 33%, which is shown by trypsinization in Figure 4. HSVEC with glycocalyx degraded by any used methods showed stronger resistance to trypsin treatment on the tested 100 W, 33% amine PP. Before glycocalyx

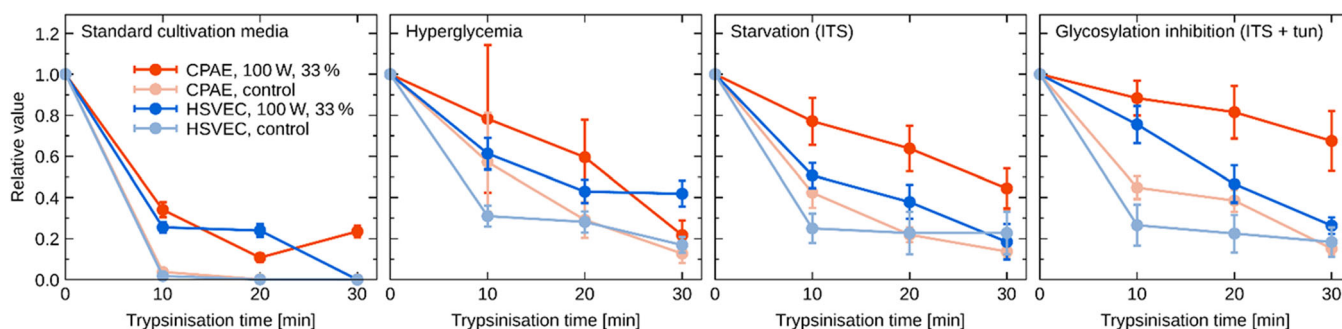


FIGURE 6 Trypsinization after degradation of thick endothelial glycocalyx by 5 h long hyperglycemia (GLU), starvation (ITS), and inhibition of glycosylation (ITS + TUN).

degradation (trypsinization in standard culture medium), about 30% of the seeded HSVEC cells remained adherent on the surface after 10 min of trypsin treatment (Figure 6). In contrast, under conditions corresponding to hyperglycemia or starvation, about 60% of the seeded cells remained adherent on the surface after 10 min of trypsin treatment. In glycosylation inhibition, it was even almost 80% of the cells. Before glycocalyx degradation on the control untreated surface, almost all HSVEC cells were detached from the surface after 10 min of trypsin treatment. However, after glycocalyx degradation by the above-mentioned methods, about 30% of the seeded HSVEC cells remained adherent on the surface after 10 min of trypsin treatment.

3.4 | Assessment of TG activity by dansyl cadaverine

The various activity of TG could also lead to the formation of different bonds to the surface. As TGs are numerous and differ among cell types, we chose a functional test—incorporation of fluorescent dansyl cadaverine by the activity of TGs. Fluorescence of cell- and surface-bound dansyl group was measured after 5 h of incubation. The TG activity showed no correlation supporting dividing cells into two groups, that is, endothelial and nonendothelial. Although the activity of TGs is the highest for VSMC (Figure 7), endothelial HSVEC cells also have a relatively high TG activity. On the other hand, both HaCaT keratinocytes nonendothelial cells and CPAE endothelial cells have lower TG activity. We can conclude that the activity of TGs is not significantly higher in exquisitely nonendothelial cells.

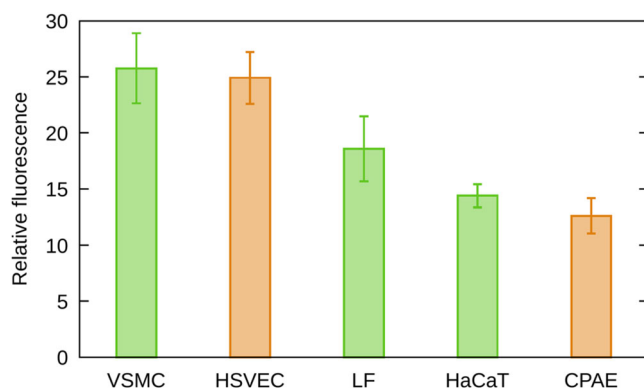


FIGURE 7 Activity of transglutaminases assessed by incorporation of fluorescent dansyl cadaverine for 5 h. Nonendothelial cells (VSMC, LF, and HaCaT) are shown in green and endothelial cells (HSVEC and CPAE) are shown in orange.

4 | DISCUSSION

The principal difference in adhesion between endothelial and nonendothelial cells should reveal why cells resist trypsin treatment. Based on previous results, the increased resistance to trypsinization of nonendothelial cells on amine PPs was explained by a nonspecific cell adhesion such as electrostatic interaction between the (negatively charged) cells and (positively charged) amino groups on the material surface.^[17,44] Compliance of endothelial cells to trypsin treatment also disproved our first hypothesis that catalytic activity of trypsin might be inhibited or blocked by the surface-bound amino groups.^[13] Nevertheless, we cannot completely exclude the possibility that the highly positively charged surfaces affect the ability of trypsin to cleave. The nonspecific binding of negatively charged domains of transmembrane proteins (including integrins) and phospholipids may lead to steric hindrance of the cleavage sites or changes in their conformation or chemical properties.^[45]

4.1 | Trypsin resistance is directly correlated to the strength of adhesion

All the cells in our previous study^[13] attach more quickly to PPs, which is more pronounced in nonendothelial, trypsin-resistant cell lines. The cell-surface interactions are governed by the physico-chemical properties of the surfaces, such as chemical functional groups, surface energy, roughness, and surface charge.^[8,46–54]

Therefore, it was assumed that this effect could be explained by the positive charge of amine PPs.^[55,56] In the current study, we found out that the surface ζ -potential is the most positive on 30 and 100 W (33%) surfaces (Figure 3a). Babaei et al.^[46] showed that the nitrogen-rich PP films acquire positive surface charge due to the presence of amino groups, whereas carboxyl groups in oxygen-rich coatings result in negative surface charges. Babaei's study examined the ζ -potential of samples with an oxygen content of about 23 at.%, and the ζ -potential reached values around -27 mV. Our carboxyl PP with a similar oxygen content exhibited more than two times higher negative ζ -potential. The layers could differ in the amount of various oxygen-containing groups, but the ζ -potential is also significantly influenced by the measurement of pH that was 7.4 in Babaei and Girard-Lauriault^[46] and 6.4 here. Babaei's samples with a nitrogen content of about 13 at.% reached ζ -potential values of $+20$ mV.^[46] This is comparable to our ζ -potential results for 100 W, 33% amine PP ($P_{av} = 33$ W), which has the ζ -potential of $+19.8$ mV. For our 30 W, 33% amine PP, the ζ -potential value was doubled.

Such a high positive ζ -potential of around +40 mV at pH 6.4 is notable as it is difficult to achieve.

Since all the studied cell types attached most quickly on the highly positive surfaces (except CPAE), surface charge likely plays an important role in the attachment rate. This hypothesis was supported by single-cell force spectroscopy, indicating that the increased short-time adhesion of cells to PPs is correlated to the amount of amino groups.^[13] The reason could be the quicker binding of ECM proteins such as fibronectin, a receptor for integrins. Fibronectin has a negative net charge in pH-neutral liquids, meaning that it could bind to a positively charged surface quickly and efficiently.^[57–59] Besides this fibronectin-integrin binding system, it is suggested that the increased attachment rate and short-time adhesion could be caused by electrostatic van der Waals attractions of positively charged surfaces and negatively charged parts of cell membranes.^[55,60–62] In addition, we confirmed that the increased trypsin resistance and quicker attachment of nonendothelial cells do not correlate with the stronger cell adhesion caused by the increased number of the particular type of cadherin or integrin molecules, that is, the strengthened focal adhesion. We performed numerous Western blottings (Supporting Information: Figure S2), but found the same level of cadherin and integrin expressions in cells growing on the control and the amine PP-coated dishes. To supplement the hypothesis that trypsin resistance of nonendothelial cells is directly associated with their increased adhesion to the amine PPs, we performed the cell scratching by AFM in the current study. It showed that VSMC (as an example of nonendothelial cells) on PP surfaces are attached stronger than HSVEC endothelial cells (Figure 5b). We can thus directly correlate trypsin resistance and the strength of cell adhesion.

4.2 | Substrate stiffness does not affect cell adhesion

Surface stiffness is an important parameter as cell-surface adhesion could be increased by increased surface stiffness due to the more active adhesion proteins.^[63,64] The ECM creates the microenvironment, which can regulate various cellular behaviors like growth, development, and death.^[65] The intimate connection between cells and the surrounding ECM allows them to react to changes in the external environment. In several studies,^[66–70] it was demonstrated that adhesion, migration, and proliferation of vascular endothelial cells (VECs) and vascular smooth muscle cells (VSMCs) were reduced on substrates with lower stiffness. Therefore, we tested the stiffness of the polymer surfaces, which was in all cases

higher than the untreated control surface. For amine PPs, there is a trend of stiffness increasing (moderately) with plasma power (Figure 3a). This result can be related to a significantly higher crosslinking of the amine PP layer deposited at higher P_{av} , as seen from the water stability of film revealed by Manakhov et al.^[22] However, even though one of the largest differences in surface stiffness is between the control surface and the carboxyl PP, they behave similarly with respect to cell trypsin resistance (Figure 4). Thus, surface stiffness can be eliminated as a key factor in the “amino-glue” effect. Furthermore, the cell stiffness is not correlated with the different adhesion of endothelial and nonendothelial cells on amine PPs nor with surface stiffness (Figure 5a).

4.3 | The activity of TGs does not affect the trypsin resistance

One of the mechanisms that mediate cell adhesion and spreading is the activity of cell surface TGs, which can crosslink cells to ECM. TGs could also act as an integrin-binding coreceptor for fibronectin and support cell adhesion in this way, and it was proved that overexpression of TGs increases cell adhesion.^[71] The increased activity of tissue TG accompanied the increased resistance to trypsinization in multiple cell lines after photodynamic therapy.^[72] All cell types studied in this work are known to express TGs. In fibroblast,^[73] VSMC,^[74] and endothelial cells TG2 is the most expressed,^[75] whereas in HaCaT it is TG1, 3, and 5.^[76] To compare their activity, we used a universal amine donor, a fluorescent monodansyl cadaverine.^[77] Dansyl fluorescence of incorporated cadaverine in washed cells served as a marker of TG activity.^[39,40] This assay showed that TGs are the most active in VSMC and LF cells, but also in the HSVEC cell line, whereas HaCaT and CPAE cells incorporated significantly less monodansyl cadaverine (Figure 7). If TGs were the cause of nonspecific binding of nonendothelial cells, then only nonendothelial cells would have higher levels of incorporated cadaverine. However, we found that TG activity in HaCaT and HSVEC does not support this hypothesis, indicating that TGs most probably do not cause the “amino-glue” effect.

4.4 | Glycocalyx degradation results in increased trypsin resistance

Endothelial cells are known to have an extremely thick, negatively charged glycocalyx, unlike nonendothelial cells. For a long time, glycocalyx was taken only as a

protective cover of the cell, but recently it was shown that it has many effects on cellular behavior.^[78] Glycocalyx affects the reorganization of cell surface receptors, including integrins, and can change their activation and thus directly affect, among other things, cell adhesion. It was shown that bulky glycocalyx could sterically restrict the efficient binding of integrins to the matrix by creating a gap.^[79] On the other hand, cells with a thick glycocalyx contain so-called “kinetic traps” created in spots where the glycocalyx is compressed, and the cytoplasmic membrane forms protrusions rich in integrin molecules.^[79] The glycocalyx is a very dynamic structure reacting to the presence of reactive oxygen and nitrogen radicals, which can be degraded and rebuilt in a few hours. Cells respond by glycocalyx degradation to many impulses such as starvation, hyperglycemia, and ischemia, and it is probably a mechanism that alters cell metabolism via integrin-mediated signaling.^[36,80,81] For this study, it is crucial that trypsin treatment destroys glycocalyx.^[82–85] The ability of trypsin to cleave cell membrane-associated protein is decelerated by bulky glycocalyx as it first has to get through its pores, and then it also has to cleave the glycocalyx to get to surface proteins.^[82,86]

Based on this knowledge, we hypothesized that nonendothelial cells bind, besides standard integrin-based mechanisms, mainly nonspecifically to positively charged PPs by all the negatively charged areas of their transmembrane proteins peeking through their thin glycocalyx and by the negatively charged membrane phospholipids.^[44,87–89] Therefore, cleavage in trypsin-specific sites does not result in efficient cell detachment. This correlates with our observation that HaCaT and VSMC cells grown on the most positively charged surface ($P_{av} = 10\text{ W}$) are the most trypsin-resistant ones.^[13] On the other hand, endothelial cells are bound mainly by their thick, negatively charged glycocalyx and by only a few spots of integrins in the kinetic traps. Trypsin treatment destroys glycocalyx and cleaves specifically bound integrins in those traps. Therefore, endothelial cells on PP surfaces detach slightly slower compared to the control surface, as it takes some time for the tensile force to break the remaining few nonspecific bonds (Figure 4).

We tested the hypothesis by degrading the glycocalyx of endothelial CPAE and HSVEC cells before trypsinization using three different methods, starvation, hyperglycemia, and inhibition of glycosylation by tunicamycin. We found that 5 h of glycocalyx degradation by all the treatments resulted in increased trypsin resistance in both tested endothelial cell lines. It was shown that cell adhesion could be increased by cell death, in particular necrosis.^[90] However, we did not observe any

morphological signs of necrosis such as swelling of cells and organelles causing an increased number and volume of cytoplasmic “vacuoles.”^[91] Thus we can exclude the impact of necrosis. The treatment of cells by tunicamycin and deprivation of glucose could also cause interruption of cell proliferation as tunicamycin leads to loss of cyclin D1. Both treatments result in the activation of ERK kinase, which leads to the stabilization of p53 and activation of p21cip1 causing G1 arrest.^[92,93] Nevertheless, the G1 arrest is noticeable only after longer treatments (at least 12 h), thus our result should not be affected.

Therefore, the results of the glycocalyx degradation experiments confirm the hypothesis. The increased resistance to trypsin treatment follows from the revealing of transmembrane proteins, which became attached to PPs the same way as in nonendothelial cells, that is, by electrostatic attraction between positive PP surface and negative parts of transmembrane proteins and phospholipids. The question remains, why do even cells grown on control (untreated) dishes show a slightly increased trypsin resistance after degradation of their glycocalyx? We can speculate that untreated endothelial cells with thick glycocalyx are more easily or quickly trypsinized as there are only integrin traps to cleave by trypsin. However, when the glycocalyx is removed, the integrins are more evenly distributed on the membrane, so it takes more time to cleave them. The increase can even be related to carboxyl groups on the surface, as the control dishes are plasma treated by the producer.^[27]

All other suggested “amino-glue” explanations, such as the effect of surface stiffness and TG activity, were excluded. We can thus conclude that the binding of endothelial cells via glycocalyx is weaker and more prone to trypsin cleavage than the binding through negatively charged parts of proteins to the positive amino groups of PPs via electrostatic attraction.

5 | CONCLUSION

The central question of this manuscript is the nature of cell adhesion to the amine and carboxyl PP surfaces. We demonstrated increased resistance to trypsin treatment observed for the nonendothelial cell lines (VSMC and HaCaT) on amine PPs, which was observed neither for endothelial cells (HSVEC and CPAE) nor on carboxyl PP. The strong attachment of nonendothelial VSMC cells was confirmed by cell scratching by AFM, which measures the total strength of integrin-mediated and nonspecific cell adhesion. Trypsin resistance could thus be correlated with the strength of cell adhesion. The mechanism of adhesion of endothelial and nonendothelial cells to

amine PPs is influenced by the action of nonspecific adhesion, especially electrostatic interactions between cells and amino functional groups. The effect of surface stiffness and TG activity were excluded as mechanisms affecting the different adhesion of endothelial and nonendothelial cells. The crucial factor is glycocalyx thickness. In nonendothelial cells with the thin glycocalyx membrane-associated proteins/glycoproteins/phospholipids, including specifically-bound integrins, protrude from the glycocalyx. They are also evenly distributed on the cell's surface and bound to the positively charged amine PP by all their negative domains. Trypsinization of exposed cleavage sites thus only makes the cell roundish, not detached. On the other hand, endothelial cells with a thick glycocalyx bind to the PPs by their negatively charged "sugar coat" as glycocalyx covers all the transmembrane proteins. There are only a few kinetic traps where glycocalyx is compressed and cytoplasmic membrane arches toward the surface to form adhesive complexes between integrins and PPs. However, trypsin can cleave both integrins in kinetic traps and glycocalyx, causing endothelial cells to detach after trypsin treatment.

AUTHOR CONTRIBUTIONS

Martina Buchtelová: Conceptualization, methodology, investigation, writing—original draft. **Lucie Blahová:** Investigation, writing—review and editing. **David Nečas:** Formal analysis, writing—review and editing, visualization. **Petra Křížková:** Methodology, investigation. **Jana Bartošiková:** Investigation. **Jiřina Medalová:** Conceptualization, methodology, investigation, writing—Original draft. **Zdeňka Kolská:** Investigation, writing—review and editing. **Dirk Hegemann:** Resources, writing—review and editing. **Lenka Zajíčková:** Conceptualization, writing—review and editing, supervision, project administration, funding acquisition.

ACKNOWLEDGMENTS

The work was supported by the Czech Science Foundation (project 21-12132J) and by the Quality Internal Grants of BUT (KInG BUT), Reg. No. CZ.02.2.69/0.0/0.0/19_073/0016948, which is financed from the OP RDE. We acknowledge CzechNanoLab Research Infrastructure supported by MEYS CR (LM2018110) and CF Nanobio-technology of CIISB, Instruct-CZ Centre, supported by MEYS CR (LM2018127). The authors would like to thank Dr. Jan Příbyl and Šimon Klimovič for their help with AFM experiments with cells.

CONFLICT OF INTEREST STATEMENT

The authors declare no conflict of interest.

DATA AVAILABILITY STATEMENT

Data that support the findings of this study are available from the corresponding author upon reasonable request.

ORCID

Dirk Hegemann  <http://orcid.org/0000-0003-4226-9326>

Lenka Zajíčková  <http://orcid.org/0000-0002-6906-8906>

REFERENCES

- [1] P. Blomstedt, *Acta Orthop.* **2014**, 85, 670.
- [2] W. T. Godbey, A. Atala, *Ann. N. Y. Acad. Sci.* **2002**, 961, 10.
- [3] R. Langer, J. P. Vacanti, *Science* **1993**, 260, 920.
- [4] A. K. Gaharwar, *Nanomaterials in Tissue Engineering: Fabrication and Applications*, Woodhead Publishing, Oxford **2013**.
- [5] Y.-P. Jiao, F.-Z. Cui, *Biomed. Mater.* **2007**, 2, R24.
- [6] H. S. Yoo, T. G. Kim, T. G. Park, *Adv. Drug Delivery Rev.* **2009**, 61, 1033.
- [7] D. Yan, J. Jones, X. Y. Yuan, X. H. Xu, J. Sheng, J. C.-M. Lee, G. Q. Ma, Q. S. Yu, *J. Biomed. Mater. Res. A* **2013**, 101, 963.
- [8] K. S. Siow, L. Britcher, S. Kumar, H. J. Griesser, *Plasma Process. Polym.* **2006**, 3, 392.
- [9] J. H. Lee, H. W. Jung, I.-K. Kang, H. B. Lee, *Biomaterials* **1994**, 15, 705.
- [10] W. Liu, J. Zhan, Y. Su, T. Wu, C. Wu, S. Ramakrishna, X. Mo, S. S. Al-Deyab, M. El-Newehy, *Colloids Surf. B* **2014**, 113, 101.
- [11] K. S. Masters, K. S. Anseth, *Advances in Chemical Engineering*, 29, Academic Press, United States, **2004**, p. 7.
- [12] D. Gradl, M. Kühl, D. Wedlich, *Mol. Cell. Biol.* **1999**, 19, 5576.
- [13] P. Černochová, L. Blahová, J. Medalová, D. Nečas, M. Michlíček, P. Kaushik, J. Příbyl, J. Bartošiková, A. Manakhov, L. Bačáková, L. Zajíčková, *Sci. Rep.* **2020**, 10, 9357.
- [14] H. Lee, S. M. Dellatore, W. M. Miller, P. B. Messersmith, *Science* **2007**, 318, 426.
- [15] K. Zhang, J. Chen, *Cell Adh. Migr.* **2012**, 6, 20.
- [16] W. E. Brown, F. Wold, *Biochemistry* **1973**, 12, 835.
- [17] M. H. Lee, D. A. Brass, R. Morris, R. J. Composto, P. Ducheyne, *Biomaterials* **2005**, 26, 1721.
- [18] M. Soler, S. Desplat-Jego, B. Vacher, L. Ponsonnet, M. Fraterno, P. Bongrand, J.-M. Martin, C. Foa, *FEBS Lett.* **1998**, 429, 89.
- [19] E. N. T. P. Bakker, A. Pistea, E. VanBavel, *J. Vasc. Res.* **2008**, 45, 271.
- [20] T. Isobe, H. Takahashi, S. Ueki, J. Takagi, Y. Saito, *Eur. J. Cell Biol.* **1999**, 78, 876.
- [21] P. B. van Wachem, C. M. Vreeriks, T. Beugeling, J. Feijen, A. Bantjes, J. P. Detmers, W. G. van Aken, *J. Biomed. Mater. Res.* **1987**, 21, 701.
- [22] A. Manakhov, M. Landová, J. Medalová, M. Michlíček, J. Polčák, D. Nečas, L. Zajíčková, *Plasma Process. Polym.* **2017**, 14, 1600123.
- [23] L. Štrbková, A. Manakhov, L. Zajíčková, A. Stoica, P. Veselý, R. Chmelík, *EMRS 2015 Symp. EE Prot. Coat. Thin Films* **2016**, 295, 70.
- [24] P. Rupper, M. Vandenbossche, L. Bernard, D. Hegemann, M. Heuberger, *Langmuir* **2017**, 33, 2340.

- [25] M. Vandenbossche, L. Petit, J. Mathon-Lagresle, F. Spano, P. Rupper, L. Bernard, D. Hegemann, *Plasma Process. Polym.* **2018**, *15*, 1700185.
- [26] D. Hegemann, I. Indutnyi, L. Zajíčková, E. Makhneva, Z. Farka, Y. Ushenin, M. Vandenbossche, *Plasma Process. Polym.* **2018**, *15*, 1800090.
- [27] I. Nemcakova, L. Blahova, P. Rysanek, A. Blanquer, L. Bacakova, L. Zajíčková, *Int. J. Mol. Sci.* **2020**, *21*, 1.
- [28] E. Makhneva, A. Manakhov, P. Skládal, L. Zajíčková, *Sel. Pap. Soc. Vac. Coaters 58th Annu. Tech. Conf.* **2016**, *290*, 116.
- [29] C. Vandenabeele, M. Buddhadasa, P.-L. Girard-Lauriault, R. Snyders, *Thin Solid Films* **2017**, *630*, 100.
- [30] A. Manakhov, P. Skládal, D. Nečas, J. Čechal, J. Polčák, M. Eliáš, L. Zajíčková, *Phys. Status Solidi* **2014**, *211*, 2801.
- [31] P. Favia, M. V. Stendardo, R. d'Agostino, *Plasm. Polym.* **1996**, *1*, 91.
- [32] Z. Kolská, *Electrokinetic Potential and Other Surface Properties of Polymer Foils and Their Modifications*, IntechOpen, Germany, Europe **2013**.
- [33] Z. Kolská, A. Řezníčková, M. Nagyová, N. Slepíčková Kasálková, P. Sajdl, P. Slepíčka, V. Švorčík, *Polym. Degrad. Stab.* **2014**, *101*, 1.
- [34] M. Michlíček, L. Blahová, E. Dvořáková, D. Nečas, L. Zajíčková, *Appl. Surf. Sci.* **2021**, *540*, 147979.
- [35] S. Wu, A. M. Näär, *PLoS One* **2019**, *14*, e0215022.
- [36] M. J. Cheng, R. Kumar, S. Sridhar, T. J. Webster, E. E. Ebong, *Int. J. Nanomed.* **2016**, *11*, 3305.
- [37] J. B. Ward, *FEBS Lett.* **1977**, *78*, 151.
- [38] S. V. Lopez-Quintero, L. M. Cancel, A. Pierides, D. Antonetti, D. C. Spray, J. M. Tarbell, *PLoS One* **2013**, *8*, e78954.
- [39] S. R. Gross, Z. Balklava, M. Griffin, *J. Invest. Dermatol.* **2003**, *121*, 412.
- [40] G. Melino, E. Candi, P. M. Steinert, *Methods in Enzymology*, Academic Press, United States, **2000**, *322*, p. 433.
- [41] H. Dvir, J. Jopp, M. Gottlieb, *J. Colloid Interface Sci.* **2006**, *304*, 58.
- [42] P. Hermanowicz, M. Sarna, K. Burda, H. Gabryś, *Rev. Sci. Instrum.* **2014**, *85*, 063703.
- [43] J. Zhong, Y. Yang, L. Liao, C. Zhang, *Biomater. Sci.* **2020**, *8*, 2734.
- [44] M. Pekker, M. N. Shneider, *J. Phys. Chem. Biophys.* **2015**, *5*, 177.
- [45] S. C. Denstman, L. E. Dillehay, J. R. Williams, *Photochem. Photobiol.* **1986**, *43*, 145.
- [46] S. Babaei, P. L. Girard-Lauriault, *Plasma Chem. Plasma Process.* **2016**, *36*, 651.
- [47] N. A. Bullett, D. P. Bullett, F.-E. Truica-Marasescu, S. Lerouge, F. Mwale, M. R. Wertheimer, *Appl. Surf. Sci.* **2004**, *235*, 395.
- [48] K. Webb, V. Hlady, P. A. Tresco, *J. Biomed. Mater. Res.* **1998**, *41*, 422.
- [49] T. G. Vladkova, *Int. J. Polym. Sci.* **2010**, *2010*, 296094.
- [50] A. A. Meyer-Plath, K. Schröder, B. Finke, A. Ohl, *Symp. Plasma Surf. Eng. Spring Meet. Ger. Phys. Soc. Regensburg. Ger* **2003**, *71*, 391.
- [51] P.-L. Girard-Lauriault, F. Mwale, M. Iordanova, C. Demers, P. Desjardins, M. R. Wertheimer, *Plasma Process. Polym.* **2005**, *2*, 263.
- [52] U. Oran, S. Swaraj, A. Lippitz, W. E. S. Unger, *Plasma Process. Polym.* **2006**, *3*, 288.
- [53] J. Friedrich, G. Kühn, R. Mix, W. Unger, *Plasma Process. Polym.* **2004**, *1*, 28.
- [54] S. Swaraj, U. Oran, A. Lippitz, J. F. Friedrich, W. E. S. Unger, *PSE 2004* **2005**, *200*, 494.
- [55] Y. Arima, H. Iwata, *J. Mater. Chem.* **2007**, *17*, 4079.
- [56] L.-P. Xu, J. Meng, S. Zhang, X. Ma, S. Wang, *Nanoscale* **2016**, *8*, 12540.
- [57] J.-H. Lin, H.-Y. Chang, W.-L. Kao, K.-Y. Lin, H.-Y. Liao, Y.-W. You, Y.-T. Kuo, D.-Y. Kuo, K.-J. Chu, Y.-H. Chu, J.-J. Shyue, *Langmuir* **2014**, *30*, 10328.
- [58] E. Lamas, R. A. Black, P. A. Mulheran, R. Tampé, R. Wieneke, O. R. T. Thomas, Z. J. Zhang, *Sci. Rep.* **2020**, *10*, 15662.
- [59] E. Lamas, K. Kubiak-Ossowska, R. A. Black, O. R. T. Thomas, Z. J. Zhang, P. A. Mulheran, *Int. J. Mol. Sci.* **2018**, *19*, 3321.
- [60] D. J. Wilkins, R. H. Ottewill, A. D. Bangham, *J. Theor. Biol.* **1962**, *2*, 165.
- [61] Y. Zhang, M. Yang, N. G. Portney, D. Cui, G. Budak, E. Ozbay, M. Ozkan, C. S. Ozkan, *Biomed. Microdevices.* **2008**, *10*, 321.
- [62] H. Hachisuka, K. Okubo, T. Karashima, M. Kusuhara, S. Nakano, O. Mori, Y. Sasai, *Kurume Med. J.* **1992**, *39*, 33.
- [63] M. J. Paszek, N. Zahir, K. R. Johnson, J. N. Lakins, G. I. Rozenberg, A. Gefen, C. A. Reinhart-King, S. S. Margulies, M. Dembo, D. Boettiger, D. A. Hammer, V. M. Weaver, *Cancer Cell* **2005**, *8*, 241.
- [64] M. S. Samuel, J. I. Lopez, E. J. McGhee, D. R. Croft, D. Strachan, P. Timpson, J. Munro, E. Schröder, J. Zhou, V. G. Brunton, N. Barker, H. Clevers, O. J. Sansom, K. I. Anderson, V. M. Weaver, M. F. Olson, *Cancer Cell* **2011**, *19*, 776.
- [65] C. Bonnans, J. Chou, Z. Werb, *Nat. Rev. Mol. Cell Biol.* **2014**, *15*, 786.
- [66] H. Chang, H. Zhang, M. Hu, J. Chen, B. Li, K. Ren, M. C. L. Martins, M. A. Barbosa, J. Ji, *Colloids Surf. B* **2017**, *149*, 379.
- [67] H. Zhang, H. Chang, L. Wang, K. Ren, M. C. L. Martins, M. A. Barbosa, J. Ji, *Biomacromolecules* **2015**, *16*, 3584.
- [68] H. Chang, H. Zhang, M. Hu, X. Chen, K. Ren, J. Wang, J. Ji, *Biomater. Sci.* **2015**, *3*, 352.
- [69] H. Chang, X. Liu, M. Hu, H. Zhang, B. Li, K. Ren, T. Boudou, C. Albiges-Rizo, C. Picart, J. Ji, *Biomacromolecules* **2016**, *17*, 2767.
- [70] H. Chang, M. Hu, H. Zhang, K. Ren, B. Li, H. Li, L. Wang, W. Lei, J. Ji, *ACS Appl. Mater. Interfaces* **2016**, *8*, 14357.
- [71] S. S. Akimov, D. Krylov, L. F. Fleischman, A. M. Belkin, *J. Cell Biol.* **2000**, *148*, 825.
- [72] D. J. Ball, S. Mayhew, D. I. Vernon, M. Griffin, S. B. Brown, *Photochem. Photobiol.* **2001**, *73*, 47.
- [73] P. Stephens, P. Grenard, P. Aeschlimann, M. Langley, E. Blain, R. Errington, D. Kipling, D. Thomas, D. Aeschlimann, *J. Cell Sci.* **2004**, *117*, 3389.
- [74] L. Faverman, L. Mikhaylova, J. Malmquist, M. Nurminskaya, *FEBS Lett.* **2008**, *582*, 1552.
- [75] R. A. Jones, B. Nicholas, S. Mian, P. J. Davies, M. Griffin, *J. Cell Sci.* **1997**, *110*, 2461.

- [76] K. Hitomi, *Eur. J. Dermatol.* **2005**, *15*, 313.
- [77] M. Akiyama, K. Sakai, T. Yanagi, S. Fukushima, H. Ihn, K. Hitomi, H. Shimizu, *Am. J. Pathol.* **2010**, *176*, 1592.
- [78] S. Reitsma, D. W. Slaaf, H. Vink, M. A. M. J. van Zandvoort, M. G. A. oude Egbrink, *Pflügers Archiv - Eur. J. Physiol.* **2007**, *454*, 345.
- [79] M. J. Paszek, C. C. Dufort, O. Rossier, R. Bainer, J. K. Mouw, K. Godula, J. E. Hudak, J. N. Lakins, A. C. Wijekoon, L. Cassereau, M. G. Rubashkin, M. J. Magbanua, K. S. Thorn, M. W. Davidson, H. S. Rugo, J. W. Park, D. A. Hammer, G. Giannone, C. R. Bertozzi, V. M. Weaver, *Nature* **2014**, *511*, 319.
- [80] M. Nieuwdorp, T. W. Van Haeften, M. C. L. G. Gouverneur, H. L. Mooij, M. H. P. Van Lieshout, M. Levi, J. C. M. Meijers, F. Holleman, J. B. L. Hoekstra, H. Vink, J. J. P. Kastelein, E. S. G. Stroes, *Diabetes* **2006**, *55*, 480.
- [81] E. C. Woods, F. Kai, J. M. Barnes, K. Pedram, M. W. Pickup, M. J. Hollander, V. M. Weaver, C. R. Bertozzi, *eLife* **2017**, *6*, e25752.
- [82] S. M. Cox, P. S. Baur, B. Haenelt, *J. Histochem. Cytochem.* **1977**, *25*, 1368.
- [83] P. Fritsch, K. Wolff, H. Hönigsmann, *J. Invest. Dermatol.* **1975**, *64*, 30.
- [84] T. Rojalin, H. J. Koster, J. Liu, R. R. Mizenko, D. Tran, S. Wachsmann-Hogiu, R. P. Carney, *ACS Sens.* **2020**, *5*, 2820.
- [85] P. Wijesekara, Y. Liu, W. Wang, E. K. Johnston, M. L. G. Sullivan, R. E. Taylor, X. Ren, *Nano Lett.* **2021**, *21*, 4765.
- [86] A. E. Altshuler, M. J. Morgan, S. Chien, G. W. Schmid-Schönbein, *Cell. Mol. Bioeng.* **2012**, *5*, 82.
- [87] A. Roosjen, H. C. van der Mei, H. J. Busscher, W. Norde, *Langmuir* **2004**, *20*, 10949.
- [88] H. J. Busscher, A. H. Weerkamp, *FEMS Microbiol. Rev.* **1987**, *3*, 165.
- [89] H. J. Busscher, M. M. Cowan, H. C. van der Mei, *FEMS Microbiol. Rev.* **1992**, *8*, 199.
- [90] H.-K. Kwon, J.-H. Lee, H.-J. Shin, J.-H. Kim, S. Choi, *Sci. Rep.* **2015**, *5*, 15623.
- [91] U. Ziegler, P. Groscurth, *Physiology* **2004**, *19*, 124.
- [92] F. Zhang, R. B. Hamanaka, E. Bobrovnikova-Marjon, J. D. Gordan, M.-S. Dai, H. Lu, M. C. Simon, J. A. Diehl, *J. Biol. Chem.* **2006**, *281*, 30036.
- [93] J. W. Brewer, L. M. Hendershot, C. J. Sherr, J. A. Diehl, *Proc. Natl. Acad. Sci. U.S.A.* **1999**, *96*, 8505.

SUPPORTING INFORMATION

Additional supporting information can be found online in the Supporting Information section at the end of this article.

How to cite this article: M. Buchtelová, L. Blahová, D. Nečas, P. Křížková, J. Bartošíková, J. Medalová, Z. Kolská, D. Hegemann, L. Zajíčková, *Plasma Processes Polym.* **2023**;20:e2200157. <https://doi.org/10.1002/ppap.202200157>